

Evolutionary walks through flower color space driven by gene expression in *Petunia* and allies (Petunieae)

Lucas C. Wheeler^{1*}, Amy Dunbar-Wallis¹, Kyle Schutz¹, Stacey D. Smith¹

1. Department of Ecology and Evolutionary Biology, University of Colorado, 1900 Pleasant Street 334 UCB, Boulder, CO, USA, 80309-0334

lwheeler9@gmail.com

Abstract

The structure and function of biochemical and developmental pathways determine the range of accessible phenotypes, which are the substrate for evolutionary change. Accordingly, we expect that observed phenotypic variation across species is strongly influenced by pathway structure, with different phenotypes arising due to changes in activity along pathway branches. Here we use flower color as a model to investigate how the structure of pigment pathways shapes the evolution of phenotypic diversity. We focus on the phenotypically diverse Petunieae clade in the nightshade family, which contains nearly 200 species of *Petunia* and related genera, as a model to understand how flavonoid pathway gene expression maps onto pigment production. We use multivariate comparative methods to estimate co-expression relationships between pathway enzymes and transcriptional regulators, and then assess how expression of these genes relates to the major axes of variation in floral pigmentation. Our results indicate that coordinated shifts in gene expression predict transitions in both total anthocyanin levels and pigment type, which, in turn, incur trade-offs with the production of UV-absorbing flavonol compounds. These findings demonstrate that the intrinsic structure of the flavonoid pathway and its regulatory architecture underlies the accessibility of pigment phenotypes and shapes evolutionary outcomes for floral pigment production.

Keywords

flavonoids, flower color, canonical correlation analysis, pathway evolution, phylo-transcriptomics, Petunieae, Solanaceae, molecular evolution, phenotypic evolution

Introduction

Biologists have long observed that species are not uniformly distributed across the space of

32 possible phenotypes, but are clustered in certain regions of the space, leaving gaps in others. One
33 explanation for this pattern is natural selection, where the clusters represent phenotypes
34 associated with some adaptive optimum (e.g. Whibley et al. 2006; Mahler et al. 2013). Another
35 contributing factor may be developmental bias, where some phenotypes are more likely
36 outcomes given the underlying genetic and developmental pathways and others are inaccessible
37 (J. M. Smith et al. 1985; Uller et al. 2018). As selection acts upon the products of development,
38 these forces may also act in concert and jointly contribute to the patchiness of phenotype space
39 (Wagner 2011).

40 While much of our understanding of the factors shaping phenotype space come from
41 experimental work (e.g. (Beldade, Koops, and Brakefield 2002; Braendle, Baer, and Félix
42 2010)), macroevolutionary approaches can also provide unique insights. For example,
43 macroevolutionary trends may mirror ontogenetic trajectories, suggesting that phenotypic
44 evolution is biased by developmental processes (Watanabe 2018). Comparative studies can also
45 be used to estimate the degree of phenotypic integration, which is tied to stronger developmental
46 bias (Jablonski 2020). Beyond purely morphological studies, the field of evo-devo has uncovered
47 numerous instances of the same genes and pathways underlying independent origins of complex
48 traits in distantly related lineages (e.g. (Xavier-Neto et al. 2007; Kozmik et al. 2008),
49 highlighting the central role of genetic and developmental pathways in shaping evolutionary
50 trajectories.

51 Here we use flower color as a model system to interrogate the relationship between
52 pathway structure and phenotypic diversity at a macroevolutionary scale. The developmental
53 basis for flower pigmentation, in particular through anthocyanin production, is arguably one of
54 the best understood pathways in plants and is widely conserved across species (Grotewold 2006;
55 Albert et al. 2014). With an extensive foundation in the genetics of anthocyanin biosynthesis, the
56 mechanisms responsible for flower color evolution have been dissected in a diverse and growing
57 list of taxa (e.g., (Des Marais and Rausher 2010; Yuan et al. 2013; Gates et al. 2018). Together
58 these studies suggest that while changes in enzyme function can contribute to flower color
59 transitions (e.g., (Ishiguro, Taniguchi, and Tanaka 2012; S. D. Smith, Wang, and Rausher 2013),
60 differences in gene expression are by far the predominant mode of color macroevolution
61 (Wessinger and Rausher 2012; Sobel and Streisfeld 2013). Nevertheless, we lack a broader
62 understanding of how the structure of the pathway combines with differential gene expression to
63 give rise to the range of observed flower pigment phenotypes and possibly explain those that are
64 not observed (Ng and Smith 2018).

65 In order to explore the role of variation in gene expression and color diversity, we focus
66 on the *Petunieae*, a clade of roughly 180 species comprising the South American genus *Petunia*
67 and eight allied genera. This group is widely known for its tremendous diversity in flower colors,
68 including white, yellow, pink, purple and red. Moreover, the cultivated petunia has long served
69 as the premier system for studying the genetics and regulation of flower color (Koes, Verweij,
70 and Quattrocchio 2005). Importantly, studies in petunia as well as other taxa have demonstrated
71 that many steps in the anthocyanin pathway are jointly regulated by a complex comprising R2R3
72 MYB, basic-helix-loop-helix (bHLH) and WD40 transcription factors (Mol, Grotewold, and
73 Koes 1998), allowing for coordinated expression of enzymes and the compounds they produce.
74 In addition to anthocyanin pigments, *Petunia* flowers also produce UV-absorbing flavonols,
75 which share biochemical precursors with anthocyanins but appear to be independently regulated
76 by different R2R3 MYBs (Sheehan et al. 2016). Changes in the expression of these transcription
77 factors and in turn their downstream targets (pathway enzymes) underlie the gain of floral UV

78 patterning (Sheehan et al. 2016), the loss of floral anthocyanins (Quattrocchio et al. 1999), and
79 the shift to red coloration (Berardi et al. 2021) in different *Petunia* species. We predict that this
80 connection between pathway gene expression and pigment variation holds across the broader
81 Petunieae clade and may explain its diversity of colors, including those beyond the range of
82 variation observed in *Petunia* itself.

83 Our study encompasses the broadest quantitative analysis of anthocyanin pigment
84 production for any flowering plant clade to-date along with pathway-wide measures of
85 expression from petal transcriptomes. Using these data, we first estimate patterns of co-
86 expression between pathway enzymes and the previously characterized classes of transcriptional
87 regulators in *Petunia*. Next, we apply morphospace approaches to characterize the pigmentation
88 space of Petunieae and identify clusters within that space. Finally, we combine these datasets to
89 determine how changes in gene expression associate with the major axes of variation in pigment
90 production. Our results demonstrate that coordinated shifts in gene expression strongly predict
91 repeated transitions from pale to intensely pigmented phenotypes and from the production of the
92 common blue pigments to the less common red and purple pigments. These coordinated changes
93 in gene expression also mediate sharp trade-offs between anthocyanins and flavonols,
94 implicating an underappreciated role of these colorless compounds in shaping visible color
95 diversity. Overall, these findings show that the structure of the pathway plays a fundamental role
96 determining the accessibility of pigment phenotypes and in turn shapes the evolutionary
97 trajectories taken to reach distinct floral pigmentation phenotypes.

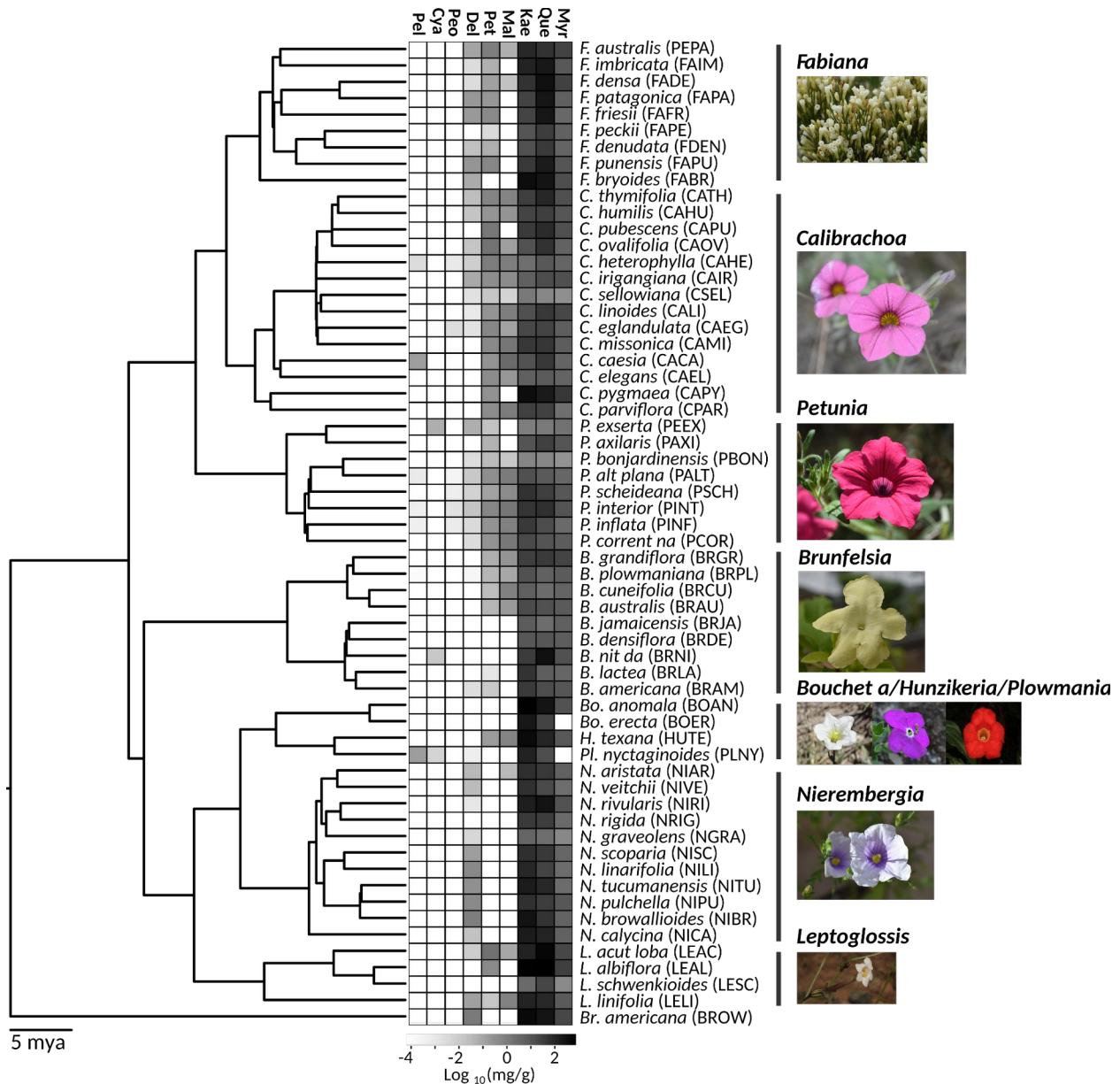
98 Results

99

100 Flower color diversity is matched by diversity of pigment profiles

101 Species of Petunieae produced all six types of anthocyanidins, the base molecules that are
102 modified to form glycosylated anthocyanins, and all three classes of the flavonol co-pigments.
103 Delphinidin and its two methylated forms (petunidin and malvidin), commonly associated with
104 blue and purple flowers (Wessinger and Rausher 2012), are the most commonly produced
105 pigments while the other three classes of pigments are only found in a few species (Fig. 1,(Ando
106 et al. 1999). The total quantity of anthocyanin pigments varies widely across species, with the
107 many white-flowered species, like *Nierembergia rigida*, producing little to no anthocyanins and
108 the deep purple and pink-flowered species, like *Calibrachoa caesia*, producing over 3 mg/g petal
109 tissue (Fig. 1; see also (Lucas C Wheeler et al. 2022)). Petunieae flowers of all colors produce
110 abundant flavonols, often at levels that are orders of magnitude higher than the anthocyanins
111 (Fig. 1, Table S1). These compounds may act as co-pigments, altering hue or intensifying the
112 color ((Holton, Brugliera, and Tanaka 1993) 3) and/or contributing to UV-patterning involved in
113 pollinator attraction (Sheehan et al. 2016).

114

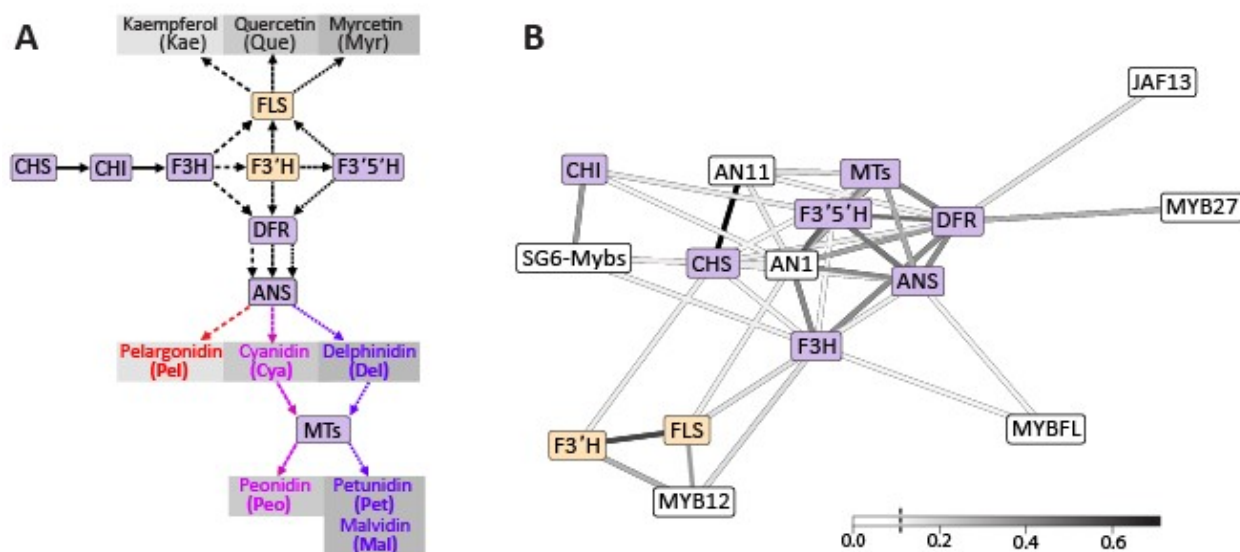


115

116 **Fig. 1. Flavonoid pigmentation varies across the Petunieae clade.** Species tree for 60
 117 taxa from Astral analysis of 3672 gene trees. Tree is rooted with *Browallia americana* as the
 118 outgroup. Heatmap shows the mean $\text{Log}_{10}(\text{mg/g})$ pigment mass fraction for the six
 119 anthocyanidins: Pelargonidin (Pel), Cyanidin (Cya), Peonidin (Peo), Delphinidin (Del),
 120 Petunidin (Pet), and Malvidin (Mal); and the three flavonols: Kaempferol (Kae), Quercetin
 121 (Que), and Myricetin (Myr). Raw values are in Table S1. Pigment level distributions are in
 122 Fig. S1. Flower images for each clade from top to bottom and left to right are as follows
 123 (with credits): *Fabiana punensis*, *Calibrachoa eglandulata*, *Petunia reitzii*, *Brunfelsia lactea*,
 124 *Nierembergia scoparia* (all by L. C. Wheeler), *Bouchetia erecta* (Edith Bergquist), *Hunzikeria*
 125 *texana* (Karla M. Benítez), *Plowmania nyctaginoides* (R. Deanna), *Nierembergia scoparia*
 126 (Lucas C. Wheeler), *Leptoglossis albiflora* (R. Deanna).

127 **Phylogenetic correlation structure reveals co-expression relationships**
 128 **across the flavonoid pathway**

129 We used petal transcriptomic data for 59 *Petunieae* species to examine clade-wide patterns of co-
 130 expression among nine enzymes and seven transcription factors of the flavonoid pathway. For
 131 this and subsequent analyses, we grouped two sets of genes, the methyl-transferases (MTs) and
 132 R2R3 MYB subgroup 6 activators, which vary in copy number across taxa but carry out similar
 133 functions (see Supplemental Text). We computed correlation coefficients, accounting for
 134 phylogenetic structure, and found two clusters of correlated structural genes, a flavonol module
 135 (F3'H and FLS) and an anthocyanin module, comprising the remaining steps of the pathway
 136 (Fig. 2). The 'late' anthocyanin biosynthesis (F3'5'H, DFR, ANS, and the MTs) form a tight
 137 cluster while the other core pathway genes (CHS and CHI) are more loosely connected. As
 138 expected, the components of the MBW complex (the SG6 MYBs, the bHLH AN1 and the WD40
 139 AN11) are mostly strongly associated with the anthocyanin module, while the flavonol regulator
 140 MYB12 (Wang et al. 2018) is co-expressed with the flavonol module. Another flavonol
 141 regulator, MYB-FL, was not co-expressed with the flavonol module, suggesting its role may be
 142 specific to the clade of *Petunia* in which it was studied (Sheehan et al. 2016). We also found the
 143 repressor MYB27 is most associated with DFR expression, consistent with the notion that it is
 144 upregulated after the late steps in the pathway to provide feedback inhibition (Albert et al. 2014).
 145 The tighter connection of AN1 to anthocyanin biosynthesis compared to the other bHLH
 146 transcription factor (JAF13) may relate to the relatively late bud stage sampled; the two bHLH
 147 genes are functionally similar but AN1 acts later in floral development (Spelt et al. 2000; Albert
 148 et al. 2014).



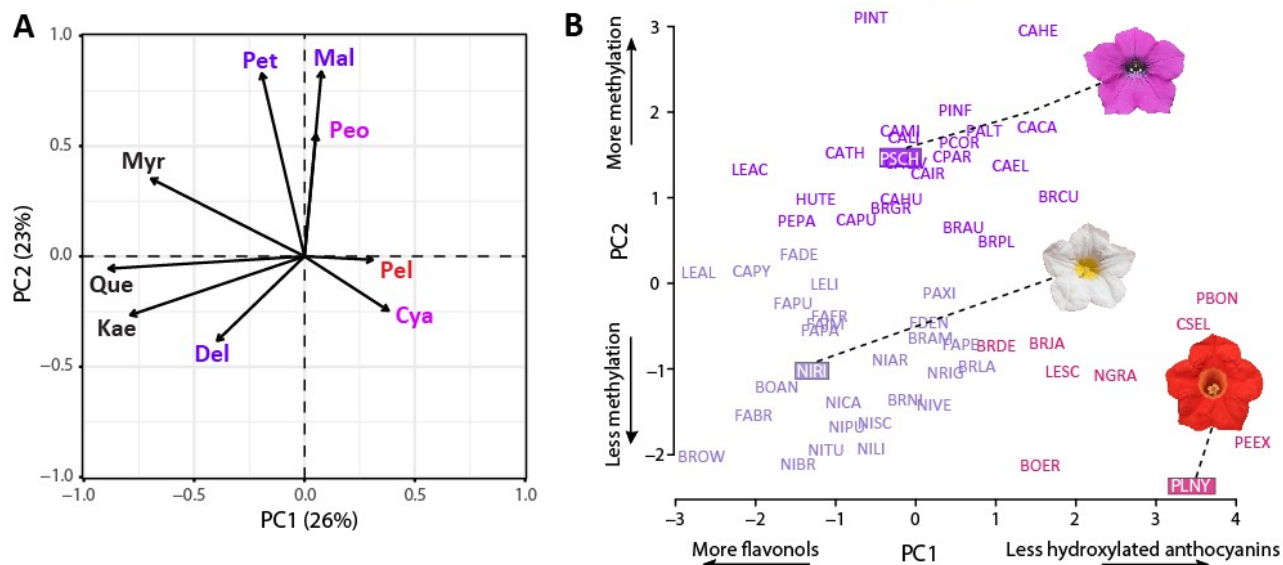
149
 150 **Fig. 2. Two clusters of co-expressed pathway genes and transcription factors.** A)
 151 Simplified flavonoid pigment pathway, focusing on the compounds found in *Petunieae* (the
 152 three flavonols and six anthocyanidins). Enzymes with multiple input/output arrows can
 153 act on multiple substrates (as indicated by the different dashed lines). Gray boxes around
 154 products indicate increasing levels of hydroxylation (left to right, mono-, di- and tri-
 155 hydroxylated). Structural genes are colored by their cluster in (B); see Table S2 for full

156 gene names. B) Correlation structure from the phylogenetic PCA of expression values for
157 structural genes (colored boxes) and transcription factors (white boxes). Values above the
158 median ($R^2 > 0.124$, indicated with a vertical $\bar{\square}$ the inset scale) were visualized with a force-
159 directed spring layout representation. Edge weights (R^2) are colored by magnitude. See Fig.
160 S2 for full matrix of correlation coefficients. Distributions of gene expression levels are
161 shown in Fig. S3.

162

163 Pigment phenotypes are divided by hydroxylation, methylation and 164 flavonoid content

165 A phylogenetic principal component analysis (pPCA) of pigment production (Fig. 1) revealed
166 sharp trade-offs among pathway branches, as manifested in the pigment profiles across species.
167 The first PC axis, which accounts for 26% of the variation, is driven by the level of
168 hydroxylation and the amount of flavonol production (Fig. 3, Table S3). It separates pale-
169 flowered species, which produce the tri-hydroxylated delphinidin and high amounts of flavonols,
170 from those which produce the less hydroxylated cyanidin and pelargonidin and lower amounts of
171 flavonols, including the bright red-flowered *Plowmania nyctaginoides* and *Petunia exserta*
172 (PLNY, PEEEX). The intensely colored purple and pink-flowered species characteristic of
173 *Petunia* and *Calibrachoa* are intermediate along this axis, with mostly tri-hydroxylated
174 anthocyanins and a range of flavonol concentrations. The second PC axis reflects the level of
175 methylation and divides the taxa that produce the unmethylated anthocyanidins (delphinidin,
176 cyanidin, pelargonidin) from those that produce mostly or entirely methylated compounds
177 (peonidin, petunidin, malvidin). We used a k-means clustering to group to the taxa in this
178 pigment profile space and recovered three clusters, the pale-flowered taxa making large amounts
179 of flavonols, the deeply pigmented taxa making methylated anthocyanidins, and the taxa making
180 less hydroxylated anthocyanidins and lower flavonols. While the first two clusters are fairly
181 uniform in color (white to light purple and deep pink to deep purple, respectively), the cluster
182 containing the diverse less hydroxylated anthocyanins and low flavonols range in color from
183 yellow (BRDE, LESC) to pink (PBON, CSEL) to red (PLNY, PEEEX).



184

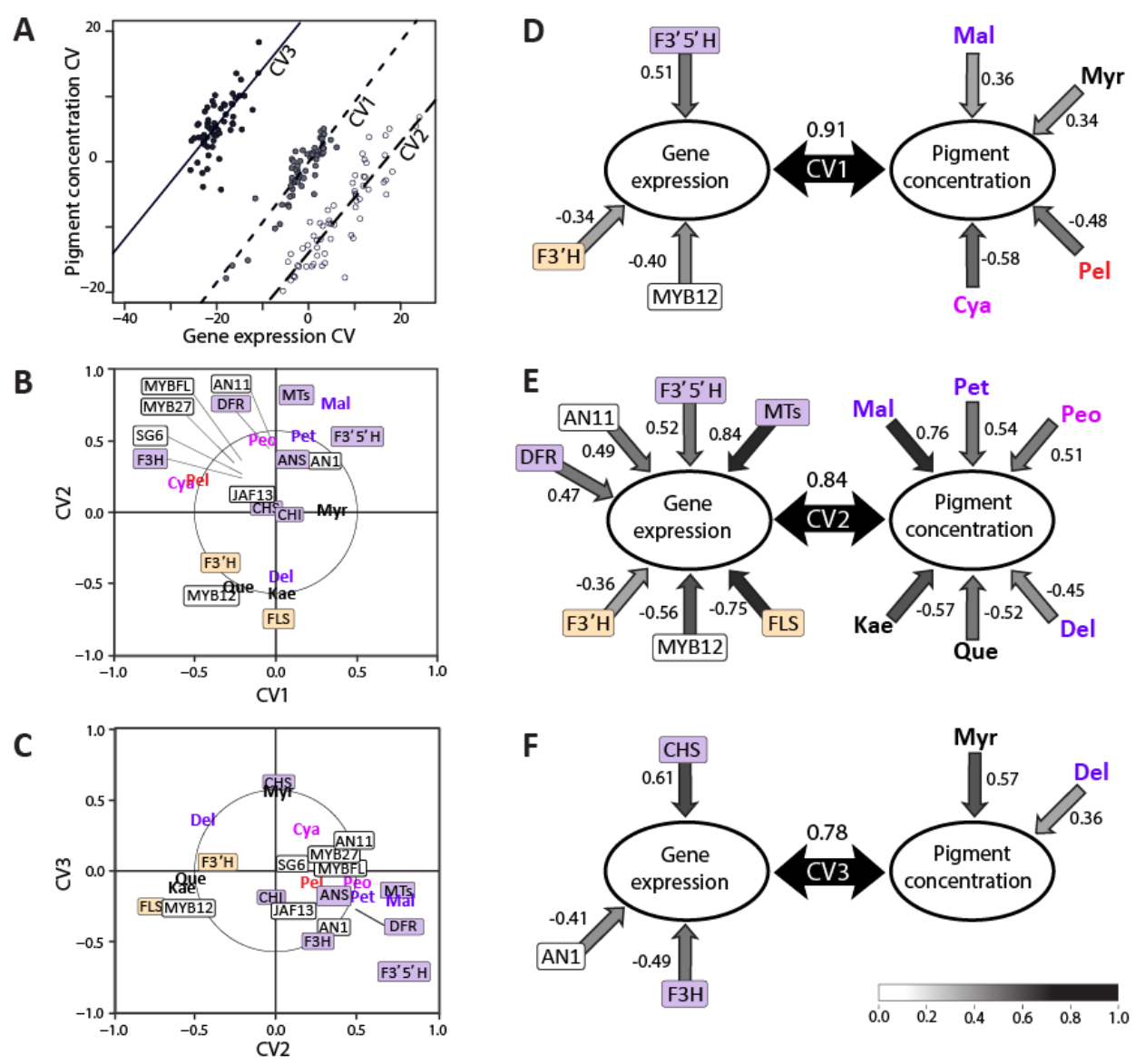
185 **Fig. 3. Clusters in pigment space defined by pathway branches.** A) Biplot from pPCA
 186 with flavonoids plotted by loading on the first two PC axes. Abbreviations follow Fig. 2. The
 187 three flavonols (quercetin, myricetin and kaempferol) plus the tri-hydroxylated delphinidin
 188 load negatively onto PC1 while the less hydroxylated pelargonidin and cyanidin load
 189 positively. The three methylated anthocyanidins (petunidin, malvidin and peonidin) load
 190 positively onto PC2. B) Species of *Petunieae* plotted by values for PC1 and PC2. Taxon
 191 labels are colored by K-means clustering. The flower of one species from each cluster is
 192 shown; taxon abbreviations follow Fig. 1.

193 Pathway gene expression predicts major pigment phenotypes

194 Phylogenetic canonical correlation analysis (pCCA) revealed a tight relationship between the
 195 expression of flavonoid pathway structural genes and regulators, and the production of flavonoid
 196 compounds. The first three canonical variates (CVs) are statistically significant and have strong
 197 correlations between gene expression and pigment concentration variables (Fig. 4). Biplots of
 198 loadings for each gene and pigment on each CV (Table S4, S5) show similar clustering patterns
 199 as recovered in the individual analyses. For example, the flavonol module corresponding to
 200 F3'H, FLS and MYB12 (Fig. 2) emerges from the pCCA (Fig. 4B, C) and groups with the two
 201 flavonols showing correlated production, quercetin and kaempferol (Fig. 3). Similarly, the three
 202 methylated anthocyanidins (peonidin, petunidin, and malvidin) group together with several of the
 203 late pathway genes (F3'5'H, ANS, MT) that control their production (Fig. 4B). Moreover, the
 204 CVs explain the expression variation underlying the major axes of pigment variation identified in
 205 the pPCA (Fig. 3). The first CV identifies genes whose expression contributes to hydroxylation
 206 level, which distinguishes the red-flowered species from the rest. Specifically, production of the
 207 less-hydroxylated pelargonidin and cyanidin is correlated with high expression of F3'H and its
 208 regulator MYB12 and low expression of F3'5'H (Fig. 4D), which diverts production towards the
 209 tri-hydroxylated compounds (Fig. 2A). The second CV explains the production of flavonols and
 210 methylated anthocyanins (Fig. 4E). Here, high expression of the methyltransferases and other
 211 late pathway genes leads to high levels of the methylated anthocyanins responsible for the
 212 intense purples and pinks as in most *Petunia* and *Calibrachoa*. Conversely, high expression of

213 the flavonol module shifts production away from anthocyanins and toward the flavonols
 214 quercetin and kaempferol, as observed in the pale and white-flowered species. Finally, the third
 215 CV addresses production of the most common anthocyanidin across the species, delphinidin, and
 216 its flavonol counterpart, the trihydroxylated myricetin. Their production appears to be shaped by
 217 expression of early genes in the pathway, which control overall flux (L C Wheeler and Smith
 218 2019).

219



220

221 **Fig. 4. Pathway gene expression correlates tightly with pigment production.** A)
 222 Scatterplot of the significant canonical variates (CVs) for pigment concentration and gene
 223 expression from phylogenetic canonical correlation analysis (phylo-CCA). The correlation
 224 coefficients for each gene expression CV and pigmentation CV are shown in C-E, inset in the
 225 black arrows. B, C) Biplots of loadings of original expression and pigment variables onto

226 CVs. For some tightly clustered variables, the location of their point is indicated with a line.
227 C, D, E) Variables with significant loadings onto each CV. Pearson correlation coefficients
228 are shown for each significant variable (expression level or pigment amount) with one-way
229 arrows. The bidirectional black arrows show the strength of the correlation between the
230 given expression and pigment CVs.

231 Relationship between pigment types and genes not broadly driven by 232 functional evolution

233 Changes in coding sequences may also contribute to the relationship between particular enzymes
234 and pathway outputs (e.g. Smith et al. 2013). For example, we might expect relaxed selection on
235 F3'5'H in lineages that have moved away from the production of tri-hydroxylated anthocyanins
236 (Wessinger and Rausher 2015). Similarly, the methyltransferases would be predicted to
237 experience strong purifying selection in the clades with high production of methylated
238 anthocyanins. We tested for relationships between the rates of non-synonymous to synonymous
239 substitutions (dN/dS) across the pathway genes and major axes of pigment variation (total
240 anthocyanins, total flavonols, fraction methylated anthocyanins, fraction tri-hydroxylated
241 delphinidin derivatives). Across these analyses, we recovered no significant correlations (Table
242 S6, Supplemental Figures S5-S8), suggesting changes at the coding level are not the primary
243 drivers of pigment variation across the species.

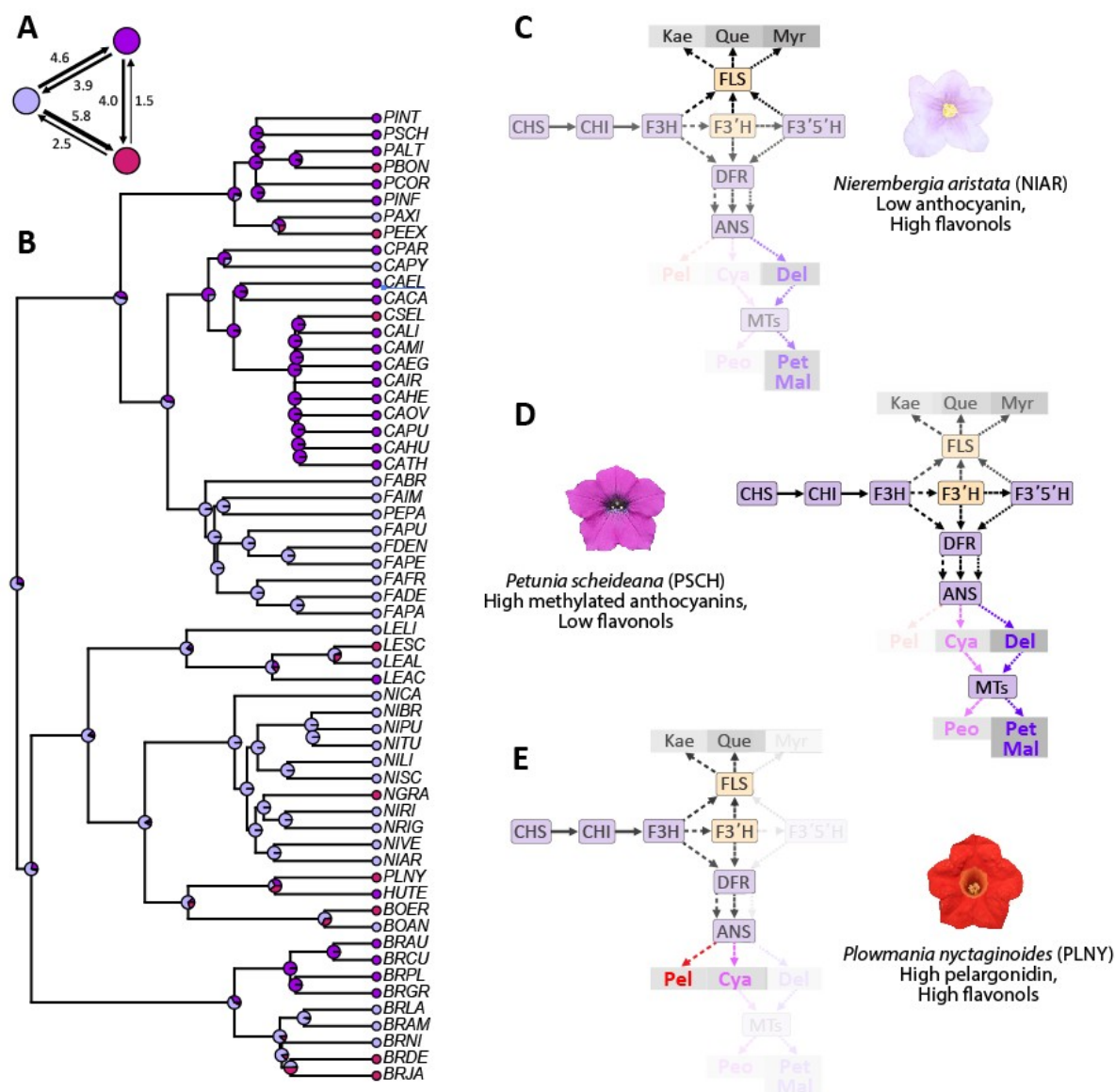
244 Nevertheless, we expect that high levels of red pelargonidin pigments should be limited
245 by the inability of *Petunia* DFR to reduce the precursor dihydrokaempferol (Forkmann and
246 Ruhnau 1987). Therefore, we examined the DFR sequence in *Plowmania nyctaginoides*, the only
247 species found to produce primarily pelargonidin (Fig. 1). Compared with other sequenced
248 Petunieae species, this species has a unique Q226K substitution (relative to *Vitis vinifera*
249 sequence positions in crystal structure 2c29) in the active site, which would be in close contact
250 with the substrate (Figure S4). This precise substitution has also been documented in a distantly
251 related red-flowered pelargonidin-producing Solanaceae species and it has been shown to
252 increase DFR activity on DHK (S. D. Smith, Wang, and Rausher 2013). Interestingly, all three
253 sequenced *P. nyctaginoides* individuals carry both the Q (CAA) and K(AAA) codons at this
254 position, suggesting that either all are heterozygous, or that there are two nearly-
255 indistinguishable DFR copies in this species (Fig. S4, Supplemental Text). All individuals are
256 fixed for a substitution Y227F, which is shared by close relatives *Bouchetia* and *Hunzikeria* (as
257 well as *Vitis vinifera*) but absent in other Petunieae species. Given its close proximity to the
258 Q226K substitution and its presence in the active site, it is possible that Y227F interacts with
259 Q226K to change the active site environment and may have played a role in a shift in DFR
260 function in *P. nyctaginoides*.

261 The deeply pigmented phenotypes are likely derived from the pale 262 colors

263 We used the phylogeny to estimate the evolutionary history of the major pigment phenotypes in
264 Petunieae. Using the best-fitting equal rates model and the pigment states from the pPCA (Fig.
265 3), we infer that the ancestor of Petunieae most likely belonged to the pale-flowered, delphinidin-
266 producing, high flavonol phenotype (p=0.7) with multiple transitions to the other phenotypes
267 (Fig. 5A, B). This pale-flowered state has been retained in *Fabiana* and *Nierembergia*, as well as
268 some *Brunfelsia* and is characterized by relatively low overall pathway expression, but high FLS

269 expression, leading to high flavonol accumulation (Fig. 5C). The intensely colored and highly
 270 methylated pink-purple phenotype is characteristic of *Petunia* and *Calibrachoa*, while the
 271 lineages that have diverged to produce less hydroxylated anthocyanins and/or lower amounts of
 272 flavonols are scattered throughout the tree, arising from ancestors of both of the other states (Fig.
 273 5A, B). The transition to producing high amounts of the tri-hydroxylated and methylated
 274 anthocyanins requires a shift to high expression of all pathway steps and typically comes at the
 275 expense of flavonol production (Fig. 4E, 5D). The red-flowered species producing less
 276 hydroxylated anthocyanins also tend to produce low amounts of flavonols (Fig. 5E).

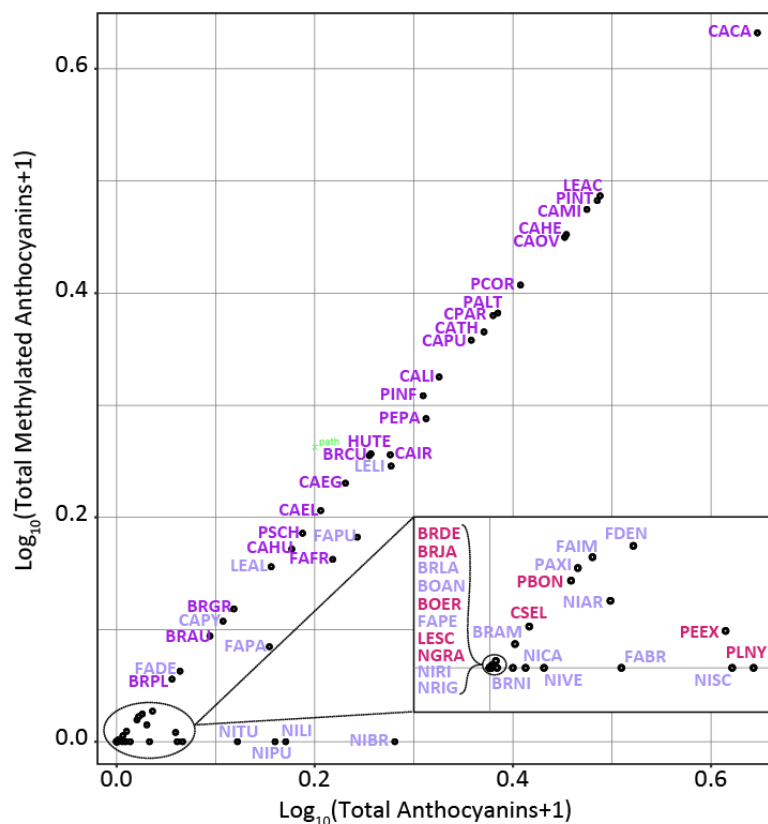
277



278
 279 **Fig. 5. Deep purple and red colors may have evolved from pale ancestors.** A)
 280 Estimated numbers of transitions between each pigment phenotype from stochastic
 281 mapping. The outgroup (*Browallia americana*) was pruned from the tree to better visualize
 282 nodes inside Petunieae. B) Maximum likelihood ancestral state estimation of the three

283 pigmentation clusters (shown in Fig. 3B). C-E) Exemplar species from each cluster. Steps of
284 the flavonoid pathway and pathway products (Fig. 2A) are shaded by their expression in
285 each, with the lower expressed branches being least visible.

286



287

288 **Fig. 6. Highest anthocyanin production in species making methylated anthocyanins.**
289 The concentration of methylated anthocyanins (mg/g) plotted against the concentration of
290 all anthocyanins. Values were $\log_{10}(X+1)$ transformed for ease of visualization. Coloring of
291 species abbreviations follows Fig. 3. Species with low anthocyanin concentrations are
292 shown in the inset portion.

293 Discussion

294

295 Our study revealed that Petunieae produce all of the six classes of anthocyanidins, including
296 three main branches (the red pelargonidin, purple cyanidin, and blue delphinidin pigments) and
297 all three methylated derivatives (Fig. 1). Although most species present only delphinidin and its
298 derivatives petunidin and malvidin, a few species are able to produce pigments down two or even
299 three branches. The UV-absorbing flavonols are present in all species, but with concentrations
300 varying over 1000-fold (Table S1, Supplemental Fig. S1). Through multivariate analyses of these
301 biochemical profiles, we found that species are clustered in pigment space by the degree of
302 hydroxylation and methylation of the anthocyanins and the extent of flavonol production. These

303 axes of variation in pigment production are tightly correlated with variation in gene expression of
304 the corresponding branches of the pathway, supporting the notion that regulatory changes are the
305 principal drivers of flower color evolution. Nevertheless, the relative rarity of species that have
306 deviated from the ancestral state of making delphinidin and delphinidin-derived anthocyanins
307 points to constraints in moving along the hue axis.
308

309

310 **Evolutionary increases in pigment intensity coupled with higher** 311 **methylation**

312

313 Changes in the amount of anthocyanin production, whether associated with continuous variation
314 in the intensity of coloration or discrete gains and losses of flower color, are common throughout
315 angiosperms (S. D. Smith and Goldberg 2015). Our phylogenetic analysis estimates four to five
316 transitions to the intensely pigmented purple phenotype, in the large genera *Petunia*,
317 *Calibrachoa*, and *Brunfelsia* as well as in *Leptoglossis* and *Hunzikeria* (Fig. 5). These flowers
318 range from hot pink, to magenta to purple, and at least for *Petunia* and *Calibrachoa* are bee-
319 pollinated (Stehmann and Semir 2001; Ando et al. 2001). The shift to producing high amounts of
320 delphinidin-derived anthocyanins is reversible in Petunieae, and several of these lineages have
321 subsequently transitioned to the two other pigment composition types (Fig. 5).

322 One unexpected finding of this study was that these convergent transitions to intense
323 pigmentation involve not only increasing flux down the delphinidin branch, but increasing
324 methylation as well (Figs. 3, 6). This pattern may relate to the co-regulation of MTs with other
325 late pathway genes (Fig. 2, (Provenzano et al. 2014). If increases in floral pigmentation often
326 occur via trans-regulatory mutations (Sobel and Streisfeld 2013), the expression of MTs may be
327 elevated together with F3'5'H, DFR and ANS, pulling flux toward petunidin and malvidin
328 production. The predominance of methylated anthocyanins in highly pigmented flowers may also
329 have effects on the color phenotype and its stability. Methylation has a reddening effect on the
330 bluish delphinidin pigments (Tanaka, Sasaki, and Ohmiya 2008), which could contribute to the
331 hot pink hues of many of these species. Moreover, methylation has important biochemical
332 properties, increasing stability and water solubility (Sarni et al. 1995; Enaru et al. 2021). These
333 factors may be particularly important as the high levels of production of anthocyanins comes at
334 the expense of flavonols (esp. quercetin and kaempferol, Fig. 4E), which can also stabilize
335 anthocyanins through intermolecular stacking (Trouillas et al. 2016).

336

337 **Limited evolutionary transitions in anthocyanin composition likely** 338 **due to ancestral preference**

339

340 Shifts in floral hue (e.g. from blue to pink) are often associated with changes in the type of
341 anthocyanin produced. Specifically, transitions from blue or purple to red commonly involve
342 shifting from more to less hydroxylated anthocyanins (reviewed in (Wessinger and Rausher

343 2012). Despite the range of colors present in Petunieae (Fig. 1), we found that such changes in
344 the level of hydroxylation are uncommon (see also (Ando et al. 1999; Ng and Smith 2018).
345 Although 10 species make detectable amounts of pelargonidin and cyanidin (Table S1), these are
346 generally present in trace amounts. The exceptions are *Petunia exserta*, which produces roughly
347 half cyanidin and half delphinidin and methylated derivatives (Berardi et al. 2021), and
348 *Plowmania nyctaginoides*, which makes 96% pelargonidin. Our phylogenetic CCA suggests that
349 the downregulation of F3'5'H is the strongest driver of shifts away from the production of
350 delphinidin-derived anthocyanins (Fig. 4D), a pattern observed in other empirical systems (e.g.
351 (S. D. Smith and Rausher 2011; Hopkins and Rausher 2011; Sánchez-Cabrera et al. 2021).
352 The fact that only two red species in Petunieae appear to have evolved red flowers via shifts to
353 less hydroxylated anthocyanins implicates other mechanisms for diversifying color. Combining
354 anthocyanins with carotenoid pigments to produce red color is a common strategy, both in
355 Solanaceae (Ng and Smith 2016) and in other taxa, such as *Mimulus* (Yuan et al. 2014).
356 Acidification of the vacuole, where anthocyanins are stored, can also shift the color to appear
357 more red (Tanaka, Sasaki, and Ohmiya 2008). This phenomenon is known in cultivars of *Petunia*
358 and *Calibrachoa* (Waterworth and Griesbach 2001), but not yet documented as part of an
359 evolutionary color transition. Finally, in addition to the reddening effect of methylation
360 mentioned above, acylation of anthocyanins has a blueing effect, so reduction in acylation can
361 also contribute to red colors (Ando et al. 1999; Berardi et al. 2021). The most deeply red
362 *Calibrachoa*, *C. sendtneriana*, is extremely rare (Stehmann et al. 1997), and although we were
363 not able to obtain replicates to include the present study, previous work demonstrates that it only
364 produces delphinidin-derivatives (Ng and Smith 2018), making it another Petunieae species to
365 produce red flowers with blue pigments. Other Petunieae with unique shades, such as the bright
366 salmon-colored *Petunia reitzii* and the burgundy *Leptoglossis acutifolia* also comprise candidates
367 for using a combination of biochemical mechanisms to produce diverse colors.

368 The rarity of shifts from producing delphinidin-derived anthocyanins to those derived
369 from pelargonidin also points to strong underlying constraints in moving along the hydroxylation
370 axis. The most likely source of such constraints is substrate specificity of multi-functional
371 pathway enzymes (e.g. DFR, ANS, Fig. 2A). The inefficiency of *Petunia hybrida* DFR in acting
372 on pelargonidin precursors has been well documented as part of efforts to breed red horticultural
373 varieties (e.g. (Gerats et al. 1982; Elomaa et al. 1995; Johnson et al. 1999). The prevalence of
374 delphinidin-derived anthocyanins across the Petunieae suggests that the preference for the
375 precursors of delphinidin is not peculiar to *P. hybrida* but likely represents the ancestral state for
376 the clade, and perhaps for the entire Solanaceae (S. D. Smith, Wang, and Rausher 2013). In this
377 context, it is notable that the only species of Petunieae to make predominantly pelargonidin,
378 *Plowmania nyctaginoides*, carries the precise single amino-acid mutation found in another red-
379 flowered lineage of Solanaceae which is known to more than double activity on the pelargonidin
380 precursor, dihydrokaempferol (Fig. S4, (S. D. Smith, Wang, and Rausher 2013)). These patterns
381 suggest that transitioning to pelargonidin production is accessible only through changes in the
382 ancestral enzyme function.

383 Conclusions

384

385 Comparative evodevo studies have the potential to reveal commonly traversed evolutionary
386 pathways and the mechanisms underlying those phenotypic shifts. Our study demonstrates that
387 *Petunia* and its close relatives have repeatedly calibrated the production of blue delphinidin-
388 derived pigments and UV-absorbing flavonols by altering levels of gene expression in the
389 anthocyanin pathway. We posit that these axes comprise evolutionary paths of least resistance,
390 whereby adjusting gene expression allows for a wide range of visible and UV-visible
391 pigmentation levels. However, expression changes are probably insufficient to overcome
392 ancestral patterns of substrate specificity in multi-functional enzymes to allow transitions along
393 the hydroxylation axis. Thus, moving beyond the range of colors accessible by changing
394 anthocyanin and flavonol levels alone likely requires novel mutations to enzyme activity and/or
395 the recruitment of additional biochemical tricks, such as vacuolar acidification, to reach new
396 color phenotypes.

397 **Methods**

398 **Transcriptome assembly**

399 We generated RNA-seq data for tissue from developing floral buds equivalent to *Petunia* bud
400 stage 5 (Pollak et al. 1993), with three replicates per species. The first replicate was the data used
401 in (Lucas C Wheeler et al. 2022), while the second and third replicates were generated using
402 RNA extracted from the buds of additional individuals collected with the same voucher (time
403 and location) as the first replicate. We generated RNA-seq libraries using the Illumina TruSeq kit
404 with IDT-for-Illumina indexes and sequenced them on an Illumina NovaSeq 6000 instrument at
405 the Weill Cornell Genomics Core Facility. For each species we combined the paired-end reads
406 from all three replicates to increase depth of coverage. To assemble *de novo* transcriptomes for
407 the 59 Petunieae species and the *Browallia americana* outgroup used in this study, we followed
408 the pipeline from (Lucas C Wheeler et al. 2022). Briefly, the pipeline carries out the following
409 steps: 1) trim the reads using IDT-for-Illumina adapter sequences, 2) perform *de novo*
410 transcriptome assembly using Trinity, 3) detect and remove chimeric sequences using the
411 run_chimera_detection.py script from (Yang and Smith 2014), 4) run Corset to cluster and
412 collapse transcripts, and 5) predict CDS using TransDecoder.

413 **Quantification of gene expression**

414 We retrieved flavonoid pathway genes and their transcription factor regulators from
415 transcriptomic CDS following the pipeline from (Lucas C Wheeler et al. 2022). Briefly, we used
416 BLASTN to identify sequences matching queries (e-value cutoff = 1e-50) for the structural
417 genes: CHS-A, CHI-A, CHI-B, F3H, FLS, F3'H, F3'5'H, DFR, ANS, MF1, MF2, and MT; the
418 transcription factors AN2, DPL, PHZ, AN11, AN1, JAF13, MYBFL, MYB27, AN4, ASR1,
419 ASR2, ASR3; and the housekeeping genes actin, tubulin, Rps18, Gapdh, Hprt. For downstream
420 analyses relating gene expression to pigment production, we included only the relevant pathway-
421 related genes and transcription factors. In contrast to the approach taken in (Lucas C Wheeler et
422 al. 2022), we did not reduce the BLAST hits to a single best match for each gene. Instead we
423 combined paralogous transcripts (e.g. CHS-A, CHS-J) into a single collective fasta reference file.
424 Because the subgroup 6 MYB activators (AN2, AN4, DPL, PHZ, ASR1, ASR2, ASR3) are
425 closely related and individual gene presence in the transcriptomes varies considerably, we also
426 combined this set of sequences into a single group SG6-Mybs (see Supplemental Text). To

427 confirm the accuracy of our gene extraction pipeline we performed a reverse BLASTN search of
428 all the resulting sequences against the annotated CDS from the *Petunia inflata* genome v1.0.1.
429 To quantify gene expression we pseudo-mapped the reads from each individual replicate
430 separately to the combined *de novo* transcriptome assembly of the corresponding species using
431 Salmon v1.5.2. To extract expression levels for the flavonoid pathway genes, we used the
432 transcript IDs from the combined fasta reference files to parse the Salmon quant.sf files and then
433 calculated a sum of expression levels for each gene by adding together the TPM values for all
434 corresponding transcripts (e.g. CHI-A and CHI-B). We then normalized the resulting summed
435 TPM values to TPM10K using the approach of (Munro et al. 2022).

436 Quantification of anthocyanin content

437 We used the same high-performance liquid chromatography (HPLC) approach to quantify the
438 mass fraction of flavonoids as in our previous *Petunieae* work ((Lucas C Wheeler et al. 2022),
439 following (Berardi et al. 2021). With the exception of a few samples that were re-run for
440 improved data quality, the anthocyanin mass fraction data is the same as that used to calculate
441 average total pigment concentration for the species in (Lucas C Wheeler et al. 2022). However,
442 we subsequently collected data for the flavonols (kaempferol, quercetin, and myricetin) in
443 corolla tissue of all replicate individuals using a similar approach. To ensure exact matching
444 between anthocyanin and flavonol samples we conducted the flavonol measurements on the
445 flavonol-containing layer remaining from the extraction protocol used to measure anthocyanin
446 content. We sampled flowers from three individuals per species and used these to calculate the
447 mean anthocyanin mass fraction (mg compound per g tissue) over replicates. For each
448 individual, we collected fresh floral corolla tissue, dried the tissue with silica gel and stored the
449 material in 2mL tubes at -80°C. For extraction of total flavonoids, we soaked 0.0005 to 0.1g of
450 dried tissue overnight in 1mL 2N HCL. We carried out acid hydrolysis of flavonoid glycosides
451 and analyzed the samples using high-performance liquid chromatography (HPLC) as in Wheeler
452 et al. (2022). Briefly, we heated samples 100-104°C for 1 hr to convert the glycosylated
453 flavonoids into their corresponding aglycones and then performed a series of liquid phase
454 extractions in ethyl acetate and isoamyl alcohol, before evaporating away excess solvent using an
455 N-EVAP apparatus and eluting in 50 µL of 1% HCl in MeOH . We injected 10 µL of sample on
456 the Agilent HPLC and separated flavonols by gradient elution on a 100-4.6 mm Chromalith
457 Performance column at 30°C using solvents A (HPLC-grade water, 0.1% trifluoroacetic acid)
458 and C (Methanol, 0.5% HCl). We analyzed all results using Agilent Chemstation software and
459 peaks were compared to standards obtained from Extrasynthese (365nm for flavonols and 520nm
460 for anthocyanidins). Resulting peak tables were individually cross-checked against
461 chromatograms and manually corrected for slight peak shifts as needed.

462 Reconstruction of species phylogeny

463 We previously followed the approach of (Walker et al. 2018) to reconstruct the species tree for
464 the *Petunieae* clade using 3,672 ortholog clusters identified from the original *de novo*
465 transcriptome assemblies as in Wheeler et al. (2022). However, for the current study, we added
466 an additional species; *Fabiana australis* (4-letter code = PEPA), which has recently been
467 renamed from *Petunia patagonica* (Alaria et al. 2022). To add *F. australis* into the analysis we
468 started with the ortholog clusters from the previous publication (downloadable from
469 <https://osf.io/b7gcp/>). We identified the best-matched sequence in the new *F. australis*
470 transcriptome using BLASTN (e-value cutoff = 1e-50), added these sequences into the clusters,

471 re-ran the cluster alignments using MAFFT, and then re-ran the species-tree analysis in Astral
472 5.7.8 using the updated clusters. We followed the TreePL smoothing approach used in (Lucas C
473 Wheeler et al. 2022) to ultrametricize the tree, using a subset of 11 genes present in all 60
474 species.

475 **Phylogenetic principal components analysis**

476 To more closely approximate normally-distributed data, we transformed the pigment mass
477 fraction (mg/g) values by applying a $\ln([mg/g \text{ pigment}] * 100) + 1$ transformation and the gene
478 expression (TPM10K) values by applying a $\ln(TPM \ 10 \ K + 1)$ transformation. We used the
479 *phyl.pca* function from the *phytools* package and the *prcomp* function from the *stats* package in
480 R v3.6.3 to perform a phylogenetic principal components analysis (pPCA) while scaling and
481 centering the transformed data. To obtain the underlying correlation matrix between transformed
482 TPM10K gene expression levels from the PCA output we extracted the covariance matrix (the *V*
483 attribute) and used the *cov2cor* function to convert it to a matrix of correlation coefficients. To
484 convert this matrix into the network shown in fig. 2 we selected all positive correlation
485 coefficients larger than the median value (0.124) and used *networkx* in Python v3.8.5 to convert
486 the matrix to a graph edge list. We generated the network figure, with edges colored according to
487 weights (correlation coefficients) using Cytoscape v3.9.1. To generate the pigment level clusters
488 shown in fig. 3, we performed K-means clustering on the first three principal components from
489 the pigment pPCA using the *kmeans* function in R with three clusters, based on visual inspection
490 of the projected data.

491 **Phylogenetic canonical correlation analysis**

492 To assess the relationships between expression of flavonoid pathway-related genes and flavonoid
493 pigment levels, we performed phylogenetic canonical correlation analysis (pCCA) on the
494 transformed data using the *phyl.cca* function in the R *phytools* package (Revell 2012). We
495 treated the gene expression levels as the “x” variable and pigment mass fraction as “y”. We used
496 the p-values calculated by *phyl.cca* to determine the statistical significance of the canonical
497 variates (CVs). We extracted the canonical coefficients from the significant CVs, which quantify
498 the coupled associations of the original pigment mass fraction and gene expression variables
499 with the corresponding multivariate CVs, and standardized them. We re-calculated the
500 significant CVs, arrayed by species ID, as the linear combination of the original variables scaled
501 by un-standardized coefficients. We then used the *cor.test* function in R to calculate each
502 canonical loading (correlation coefficients of original variables with their corresponding CV) and
503 cross-loading (correlation coefficients of original variables with the CV for the other data block;
504 e.g. pigment levels with gene expression CV1) with corresponding p-values.

505 **Stochastic mapping and ancestral state estimation**

506 We used the stochastic mapping tools in *phytools* to estimate the number of transitions between
507 each pigment phenotype using 200 simulations of character history. We also used the *ace*
508 function in *phytools* to estimate ancestral states across the tree. For both analyses, we used an
509 equal rates model, as the all-rates-different model did not provide a significantly better fit to the
510 data.

511 **Molecular evolution**

512 We extracted a single best-matched sequence for each gene from each species using the approach
513 of (Lucas C Wheeler et al. 2022) and used HyPhy to fit a free-rates dN/dS model that allows a
514 separate dN/dS ratio for each tip. We then extracted dN/dS trees from the HyPhy output and
515 calculated a root-to-tip dN/dS ratio for each tip. We assessed the relationships between these
516 values and the principal axes of flavonoid variation using linear regression (for details see
517 Supplemental Text).

518 **Acknowledgments**

519 This work utilized the RMACC Summit and Alpine supercomputer. Summit is a joint effort of
520 the University of Colorado Boulder and Colorado State University, supported by the National
521 Science Foundation (awards ACI-1532235 and ACI-1532236), the University of Colorado
522 Boulder, and Colorado State University. Alpine is jointly funded by the University of Colorado
523 Boulder, the University of Colorado Anschutz, Colorado State University, and the National
524 Science Foundation (award 2201538).

525 **Funding**

526 This work was funded by NSF-DEB 1553114 to SDS. The funders had no role in study design,
527 data collection, analysis, decision to publish, or manuscript preparation.

528 **Availability of data and materials**

529 The transcriptome assemblies, scripts, and processed data files used to conduct the analyses are
530 available in the supplementary OSF repo (<https://osf.io/zg9cu/>). The raw RNA-seq data files
531 have been added to the existing SRA BioProject PRJNA746328.

532 **Author contributions**

533 SDS and LCW conceived the study and outlined the experimental design. LCW and SDS
534 developed the analyses. ADW and LCW performed HPLC. LCW reconstructed the species
535 phylogeny based on previous work. LCW built the sequencing libraries and assembled the *de*
536 *novo* transcriptomes. LCW and SDS conducted the statistical analyses of the data and drafted the
537 manuscript with revisions from ADW. KS undertook careful curation of the HPLC raw data.

538 **Competing interests**

539 The authors declare that they have no competing interests.

540

- Alaria, Alejandrina, John H. Chau, Richard G. Olmstead, and Iris E. Peralta. 2022. "Relationships among Calibrachoa, Fabiana and Petunia (Petunieae Tribe, Solanaceae) and a New Generic Placement of Argentinean Endemic Petunia Patagonica." *PhytoKeys* 194 (April): 75–93. <https://doi.org/10.3897/phytokeys.194.68404>.
- Albert, Nick W., Kevin M. Davies, David H. Lewis, Huaibi Zhang, Mirco Montefiori, Cyril Brendolise, Murray R. Boase, Hanh Ngo, Paula E. Jameson, and Kathy E. Schwinn. 2014. "A Conserved Network of Transcriptional Activators and Repressors Regulates Anthocyanin Pigmentation in Eudicots." *The Plant Cell*, March, tpc.113.122069. <https://doi.org/10.1105/tpc.113.122069>.
- Ando, Toshio, Masashi Nomura, Jun Tsukahara, Hitoshi Watanabe, Hisashi Kokubun, Tatsuya Tsukamoto, Goro Hashimoto, Eduardo Marchesi, and Ian J. Kitching. 2001. "Reproductive Isolation in a Native Population of Petunia Sensu Jussieu (Solanaceae)." *Annals of Botany* 88 (3): 403–13. <https://doi.org/10.1006/anbo.2001.1485>.
- Ando, Toshio, Norio Saito, Fumi Tatsuzawa, Tomoko Kakefuda, Keiko Yamakage, Etsuko Ohtani, Maya Koshi-ishi, et al. 1999. "Floral Anthocyanins in Wild Taxa of Petunia (Solanaceae)." *Biochemical Systematics and Ecology* 27 (6): 623–50. [https://doi.org/10.1016/S0305-1978\(98\)00080-5](https://doi.org/10.1016/S0305-1978(98)00080-5).
- Beldade, Patrícia, Kees Koops, and Paul M. Brakefield. 2002. "Developmental Constraints versus Flexibility in Morphological Evolution." *Nature* 416 (6883): 844–47. <https://doi.org/10.1038/416844a>.
- Berardi, Andrea E, Korinna Esfeld, Lea Jäggi, Therese Mandel, Gina M Cannarozzi, and Cris Kuhlemeier. 2021. "Complex Evolution of Novel Red Floral Color in Petunia." *The Plant Cell*, no. koab114 (April). <https://doi.org/10.1093/plcell/koab114>.
- Braendle, Christian, Charles F. Baer, and Marie-Anne Félix. 2010. "Bias and Evolution of the Mutationally Accessible Phenotypic Space in a Developmental System." *PLOS Genetics* 6 (3): e1000877. <https://doi.org/10.1371/journal.pgen.1000877>.
- Des Marais, David L., and Mark D. Rausher. 2010. "PARALLEL EVOLUTION AT MULTIPLE LEVELS IN THE ORIGIN OF HUMMINGBIRD POLLINATED FLOWERS IN *IPOMOEA*." *Evolution*, March. <https://doi.org/10.1111/j.1558-5646.2010.00972.x>.
- Elomaa, Paula, Yrjö Helariutta, Mika Kotilainen, Teemu H. Teeri, Robert J. Griesbach, and Pauli Seppänen. 1995. "Transgene Inactivation In Petunia Hybrida Is Influenced by the Properties of the Foreign Gene." *Molecular and General Genetics MGG* 248 (6): 649–56. <https://doi.org/10.1007/BF02191704>.
- Enaru, Bianca, Georgiana Dreţcanu, Teodora Daria Pop, Andreea Stănilă, and Zorița Diaconeasa. 2021. "Anthocyanins: Factors Affecting Their Stability and Degradation." *Antioxidants* 10 (12): 1967. <https://doi.org/10.3390/antiox10121967>.
- Forkmann, G., and B. Ruhnau. 1987. "Distinct Substrate Specificity of Dihydroflavonol 4-Reductase from Flowers of Petunia Hybrida." *Zeitschrift Für Naturforschung C* 42 (9–10): 1146–48. <https://doi.org/10.1515/znc-1987-9-1026>.
- Gates, Daniel J., Bradley J. S. C. Olson, Tom E. Clemente, and Stacey D. Smith. 2018. "A Novel

- R3 MYB Transcriptional Repressor Associated with the Loss of Floral Pigmentation in *Iochroma*.” *New Phytologist* 217 (3): 1346–56.
<https://doi.org/10.1111/nph.14830>.
- Gerats, A. G. M., P. de Vlaming, M. Doodeman, B. Al, and A. W. Schram. 1982. “Genetic Control of the Conversion of Dihydroflavonols into Flavonols and Anthocyanins in Flowers of *Petunia Hybrida*.” *Planta* 155 (4): 364–68.
<https://doi.org/10.1007/BF00429466>.
- Grotewold, Erich. 2006. “The Genetics and Biochemistry of Floral Pigments.” *Annual Review of Plant Biology* 57: 761–80.
<https://doi.org/10.1146/annurev.arplant.57.032905.105248>.
- Holton, Timothy A., Filippa Brugliera, and Yoshikazu Tanaka. 1993. “Cloning and Expression of Flavonol Synthase from *Petunia Hybrida*.” *The Plant Journal* 4 (6): 1003–10. <https://doi.org/10.1046/j.1365-313X.1993.04061003.x>.
- Hopkins, Robin, and Mark D. Rausher. 2011. “Identification of Two Genes Causing Reinforcement in the Texas Wildflower *Phlox Drummondii*.” *Nature* 469 (7330): 411. <https://doi.org/10.1038/nature09641>.
- Ishiguro, Kanako, Masumi Taniguchi, and Yoshikazu Tanaka. 2012. “Functional Analysis of *Antirrhinum Kelloggii* Flavonoid 3'-Hydroxylase and Flavonoid 3',5'-Hydroxylase Genes; Critical Role in Flower Color and Evolution in the Genus *Antirrhinum*.” *Journal of Plant Research* 125 (3): 451–56. <https://doi.org/10.1007/s10265-011-0455-5>.
- Jablonski, David. 2020. “Developmental Bias, Macroevolution, and the Fossil Record.” *Evolution & Development* 22 (1–2): 103–25. <https://doi.org/10.1111/ede.12313>.
- Johnson, Eric T., Hankuil Yi, Byongchul Shin, Boung-Jun Oh, Hyeonsook Cheong, and Giltsu Choi. 1999. “*Cymbidium Hybrida* Dihydroflavonol 4-Reductase Does Not Efficiently Reduce Dihydrokaempferol to Produce Orange Pelargonidin-Type Anthocyanins.” *The Plant Journal* 19 (1): 81–85. <https://doi.org/10.1046/j.1365-313X.1999.00502.x>.
- Koes, Ronald, Walter Verweij, and Francesca Quattrocchio. 2005. “Flavonoids: A Colorful Model for the Regulation and Evolution of Biochemical Pathways.” *Trends in Plant Science*, Special Issue: Plant model systems, 10 (5): 236–42.
<https://doi.org/10.1016/j.tplants.2005.03.002>.
- Kozmik, Zbynek, Jana Ruzickova, Kristyna Jonasova, Yoshifumi Matsumoto, Pavel Vopalensky, Iryna Kozmikova, Hynek Strnad, et al. 2008. “Assembly of the Cnidarian Camera-Type Eye from Vertebrate-like Components.” *Proceedings of the National Academy of Sciences* 105 (26): 8989–93.
<https://doi.org/10.1073/pnas.0800388105>.
- Mahler, D. Luke, Travis Ingram, Liam J. Revell, and Jonathan B. Losos. 2013. “Exceptional Convergence on the Macroevolutionary Landscape in Island Lizard Radiations.” *Science* 341 (6143): 292–95. <https://doi.org/10.1126/science.1232392>.
- Mol, Joseph, Erich Grotewold, and Ronald Koes. 1998. “How Genes Paint Flowers and Seeds.” *Trends in Plant Science* 3 (6): 212–17. [https://doi.org/10.1016/S1360-1385\(98\)01242-4](https://doi.org/10.1016/S1360-1385(98)01242-4).
- Munro, Catriona, Felipe Zapata, Mark Howison, Stefan Siebert, and Casey W Dunn. 2022. “Evolution of Gene Expression across Species and Specialized Zooids in Siphonophora.” *Molecular Biology and Evolution* 39 (2): msac027.

- <https://doi.org/10.1093/molbev/msac027>.
- Ng, Julienne, and Stacey D. Smith. 2016. "How to Make a Red Flower: The Combinatorial Effect of Pigments." *AoB PLANTS* 8 (January).
<https://doi.org/10.1093/aobpla/plw013>.
- . 2018. "Why Are Red Flowers so Rare? Testing the Macroevolutionary Causes of Tippiness." *Journal of Evolutionary Biology* 31 (12): 1863–75.
<https://doi.org/10.1111/jeb.13381>.
- Pollak, P. E., T. Vogt, Y. Mo, and L. P. Taylor. 1993. "Chalcone Synthase and Flavonol Accumulation in Stigmas and Anthers of *Petunia hybrida*." *Plant Physiology* 102 (3): 925–32. <https://doi.org/10.1104/pp.102.3.925>.
- Provenzano, Sofia, Cornelis Spelt, Satoko Hosokawa, Noriko Nakamura, Filippa Brugliera, Linda Demelis, Daan P. Geerke, et al. 2014. "Genetic Control and Evolution of Anthocyanin Methylation." *Plant Physiology* 165 (3): 962–77.
<https://doi.org/10.1104/pp.113.234526>.
- Quattrocchio, F, J Wing, K van der Woude, E Souer, N de Vetten, J Mol, and R Koes. 1999. "Molecular Analysis of the Anthocyanin2 Gene of *Petunia* and Its Role in the Evolution of Flower Color." *The Plant Cell* 11 (8): 1433–44.
- Revell, Liam J. 2012. "Phytools: An R Package for Phylogenetic Comparative Biology (and Other Things)." *Methods in Ecology and Evolution* 3 (2): 217–23.
<https://doi.org/10.1111/j.2041-210X.2011.00169.x>.
- Sánchez-Cabrera, Mercedes, Francisco Javier Jiménez-López, Eduardo Narbona, Montserrat Arista, Pedro L. Ortiz, Francisco J. Romero-Campero, Karolis Ramanauskas, Boris Igić, Amelia A. Fuller, and Justen B. Whittall. 2021. "Changes at a Critical Branchpoint in the Anthocyanin Biosynthetic Pathway Underlie the Blue to Orange Flower Color Transition in *Lysimachia arvensis*." *Frontiers in Plant Science* 12.
<https://www.frontiersin.org/articles/10.3389/fpls.2021.633979>.
- Sarni, Pascale, H el ene Fulcrand, V eronique Souillol, Jean-Marc Souquet, and V eronique Cheynier. 1995. "Mechanisms of Anthocyanin Degradation in Grape Must-like Model Solutions." *Journal of the Science of Food and Agriculture* 69 (3): 385–91.
<https://doi.org/10.1002/jsfa.2740690317>.
- Sheehan, Hester, Michel Moser, Ulrich Klahre, Korinna Esfeld, Alexandre Dell’Olivo, Therese Mandel, Sabine Metzger, Michiel Vandenbusche, Loreta Freitas, and Cris Kuhlemeier. 2016. "MYB-FL Controls Gain and Loss of Floral UV Absorbance, a Key Trait Affecting Pollinator Preference and Reproductive Isolation." *Nature Genetics* 48 (2): 159–66. <https://doi.org/10.1038/ng.3462>.
- Smith, J. Maynard, R. Burian, S. Kauffman, P. Alberch, J. Campbell, B. Goodwin, R. Lande, D. Raup, and L. Wolpert. 1985. "Developmental Constraints and Evolution: A Perspective from the Mountain Lake Conference on Development and Evolution." *The Quarterly Review of Biology* 60 (3): 265–87. <https://doi.org/10.1086/414425>.
- Smith, Stacey D., and Emma E. Goldberg. 2015. "Tempo and Mode of Flower Color Evolution." *American Journal of Botany* 102 (7): 1014–25.
<https://doi.org/10.3732/ajb.1500163>.
- Smith, Stacey D., and Mark D. Rausher. 2011. "Gene Loss and Parallel Evolution Contribute to Species Difference in Flower Color." *Molecular Biology and Evolution* 28 (10): 2799–2810. <https://doi.org/10.1093/molbev/msr109>.
- Smith, Stacey D., Shunqi Wang, and Mark D. Rausher. 2013. "Functional Evolution of an

- Anthocyanin Pathway Enzyme during a Flower Color Transition.” *Molecular Biology and Evolution* 30 (3): 602–12. <https://doi.org/10.1093/molbev/mss255>.
- Sobel, James M., and Matthew A. Streisfeld. 2013. “Flower Color as a Model System for Studies of Plant Evo-Devo.” *Frontiers in Plant Science* 4: 321. <https://doi.org/10.3389/fpls.2013.00321>.
- Spelt, Cornelis, Francesca Quattrocchio, Joseph N. M. Mol, and Ronald Koes. 2000. “Anthocyanin1 of Petunia Encodes a Basic Helix-Loop-Helix Protein That Directly Activates Transcription of Structural Anthocyanin Genes.” *The Plant Cell* 12 (9): 1619–31. <https://doi.org/10.1105/tpc.12.9.1619>.
- Stehmann, João Renato, and João Semir. 2001. “Biologia reprodutiva de Calibrachoa elegans (Miers) Stehmann & Semir (Solanaceae).” *Brazilian Journal of Botany* 24 (March): 43–49. <https://doi.org/10.1590/S0100-84042001000100005>.
- Stehmann, João Renato, João Semir, Joao Renato Stehmann, and Joao Semir. 1997. “A New Species and New Combinations in Calibrachoa (Solanaceae).” *Novon* 7 (4): 417. <https://doi.org/10.2307/3391775>.
- Tanaka, Yoshikazu, Nobuhiro Sasaki, and Akemi Ohmiya. 2008. “Biosynthesis of Plant Pigments: Anthocyanins, Betalains and Carotenoids.” *The Plant Journal* 54 (4): 733–49. <https://doi.org/10.1111/j.1365-313X.2008.03447.x>.
- Trouillas, Patrick, Juan C. Sancho-García, Victor De Freitas, Johannes Gierschner, Michal Otyepka, and Olivier Dangles. 2016. “Stabilizing and Modulating Color by Copigmentation: Insights from Theory and Experiment.” *Chemical Reviews* 116 (9): 4937–82. <https://doi.org/10.1021/acs.chemrev.5b00507>.
- Uller, Tobias, Armin P Moczek, Richard A Watson, Paul M Brakefield, and Kevin N Laland. 2018. “Developmental Bias and Evolution: A Regulatory Network Perspective.” *Genetics* 209 (4): 949–66. <https://doi.org/10.1534/genetics.118.300995>.
- Wagner, Andreas. 2011. *The Origins of Evolutionary Innovations: A Theory of Transformative Change in Living Systems*. OUP Oxford.
- Walker, Joseph F., Ya Yang, Tao Feng, Alfonso Timoneda, Jessica Mikenas, Vera Hutchison, Caroline Edwards, et al. 2018. “From Cacti to Carnivores: Improved Phylotranscriptomic Sampling and Hierarchical Homology Inference Provide Further Insight into the Evolution of Caryophyllales.” *American Journal of Botany* 105 (3): 446–62. <https://doi.org/10.1002/ajb2.1069>.
- Watanabe, Junya. 2018. “Clade-Specific Evolutionary Diversification along Ontogenetic Major Axes in Avian Limb Skeleton.” *Evolution* 72 (12): 2632–52. <https://doi.org/10.1111/evo.13627>.
- Waterworth, Rebeccah A., and Robert J. Griesbach. 2001. “The Biochemical Basis for Flower Color in Calibrachoa.” *HortScience* 36 (1): 131–32. <https://doi.org/10.21273/HORTSCI.36.1.131>.
- Wessinger, Carolyn A., and Mark D. Rausher. 2012. “Lessons from Flower Colour Evolution on Targets of Selection.” *Journal of Experimental Botany* 63 (16): 5741–49. <https://doi.org/10.1093/jxb/ers267>.
- . 2015. “Ecological Transition Predictably Associated with Gene Degeneration.” *Molecular Biology and Evolution* 32 (2): 347–54. <https://doi.org/10.1093/molbev/msu298>.
- Wheeler, L C, and S D Smith. 2019. “Computational Modeling of Anthocyanin Pathway Evolution: Biases, Hotspots, and Trade-Offs.” *Integrative and Comparative Biology*,

- May, icz049. <https://doi.org/10.1093/icb/icz049>.
- Wheeler, Lucas C, Joseph F Walker, Julianne Ng, Rocío Deanna, Amy Dunbar-Wallis, Alice Backes, Pedro H Pezzi, et al. 2022. "Transcription Factors Evolve Faster Than Their Structural Gene Targets in the Flavonoid Pigment Pathway." *Molecular Biology and Evolution* 39 (3): msac044. <https://doi.org/10.1093/molbev/msac044>.
- Whibley, Annabel C., Nicolas B. Langlade, Christophe Andalo, Andrew I. Hanna, Andrew Bangham, Christophe Thébaud, and Enrico Coen. 2006. "Evolutionary Paths Underlying Flower Color Variation in *Antirrhinum*." *Science* 313 (5789): 963–66. <https://doi.org/10.1126/science.1129161>.
- Xavier-Neto, J., R. A. Castro, A. C. Sampaio, A. P. Azambuja, H. A. Castillo, R. M. Cravo, and M. S. Simões-Costa. 2007. "Cardiovascular Development: Towards Biomedical Applicability." *Cellular and Molecular Life Sciences* 64 (6): 719. <https://doi.org/10.1007/s00018-007-6524-1>.
- Yang, Ya, and Stephen A. Smith. 2014. "Orthology Inference in Nonmodel Organisms Using Transcriptomes and Low-Coverage Genomes: Improving Accuracy and Matrix Occupancy for Phylogenomics." *Molecular Biology and Evolution* 31 (11): 3081–92. <https://doi.org/10.1093/molbev/msu245>.
- Yuan, Yao-Wu, Janelle M. Sagawa, Laura Frost, James P. Vela, and Harvey D. Bradshaw Jr. 2014. "Transcriptional Control of Floral Anthocyanin Pigmentation in Monkeyflowers (*Mimulus*)." *New Phytologist* 204 (4): 1013–27. <https://doi.org/10.1111/nph.12968>.
- Yuan, Yao-Wu, Janelle M Sagawa, Riane C Young, Brian J Christensen, and Harvey D Bradshaw Jr. 2013. "Genetic Dissection of a Major Anthocyanin QTL Contributing to Pollinator-Mediated Reproductive Isolation Between Sister Species of *Mimulus*." *Genetics* 194 (1): 255–63. <https://doi.org/10.1534/genetics.112.146852>.